

In-Vitro Bioactivity Evaluation of Hydrangenol Extracted from *Hydrangea macrophylla* (Thunb.) Ser. Leaves

Ahlam Al-Yafeai¹, Barbara Schmitt¹, Angelika Malarski¹, Volker Böhm^{1,*}

¹Friedrich Schiller University Jena, Institute of Nutritional Sciences, 07743 Jena, Germany

ARTICLE HISTORY

Received: Nov. 21, 2023

Accepted: Jan. 06, 2024

KEYWORDS

Antioxidant activity,
TEAC,
ORAC,
Anti-diabetic potential,
Inhibition of enzymatic
browning.

Abstract: *Hydrangea macrophylla* plant, native to Japan and Korea, has been attracting scientific attention due to its potential applications in both food science and health-related research. In this investigation, dry *Hydrangea* leaves were utilized as the source material. Subsequent to comminution and thermal treatment at 70 °C for an 18-hour duration, followed by a 30-minute ultrasonic bath extraction and a 5-minute centrifugation at 5000 rpm, hydrangenol was isolated through preparative HPLC. The investigation involved assessing the antioxidant capacity of hydrangenol, its impact on the activity of α -amylase and α -glucosidase enzymes, and its ability to prevent enzymatic browning. Quantification of antioxidant capacity, determined through TEAC (Trolox Equivalent Antioxidant Capacity), showed values from 1.8 to 3.2 mmol TE/mmol. Likewise, the ORAC (Oxygen Radical Absorbance Capacity) values were in the range of 16.5-27.0 mmol TE/mmol. Total phenolics content (Folin-Ciocalteu test) yielded a range of 7.1-11.2 g GAE (Gallic Acid Equivalents) per 100 g. Examining α -amylase inhibition, hydrangenol demonstrated a 52% inhibition (IC₅₀: 3.6 mg/mL), whereas acarbose (positive control) displayed a higher inhibition of 99 % (IC₅₀: 0.51 mg/mL). Regarding α -glucosidase inhibition, hydrangenol exhibited a 51% inhibition (IC₅₀: 0.97 mg/mL), while acarbose displayed a 46% inhibition (IC₅₀: 2.1 mg/mL). Additionally, the activity of PPO was suppressed by 61% at hydrangenol concentrations of 1 mg/mL and 2 mg/mL, and by 46% at a concentration of 4 mg/mL.

1. INTRODUCTION

Recent advances in health and nutrition have sparked a renewed fascination with natural compounds possessing antioxidant properties. A diet abundant in these antioxidants holds the potential to positively impact human health, lowering the risk of ailments such as cardiovascular diseases, cancers, and age-related macular degeneration (Singh & Goyal, 2008). Phenolic compounds, commonly referred to as polyphenols, are remarkable secondary metabolites synthesized by plants. They are characterized by the presence of one or more phenolic rings with attached hydroxyl groups. These structurally diverse compounds originate from plant pathways such as pentose phosphate, shikimate, and phenylpropanoid (Gianmaria *et al.*, 2011). Polyphenols can be categorized into specific groups based on the strength of their phenolic

*CONTACT: Volker Böhm ✉ Volker.Boehm@uni-jena.de 📍 Friedrich Schiller University Jena, Institute of Nutritional Sciences, 07743 Jena, Germany

rings, which encompass phenolic acids, flavonoids, stilbenes, and lignans (Abbas *et al.*, 2017). *Hydrangea macrophylla* subsp. *serrata* (Thunb.) is a deciduous shrub native to Japan and Korea, known for its historical use in making Amacha, a ceremonial tea that derives its name from the Japanese words "甘" for sweet and "茶" for tea (Moll *et al.*, 2022). The fermentation process applied to its leaves enhances sweetness by increasing the content of the aglycon phylloidalin, contributing to the unique flavor of this traditional tea, often referred to as "tea-hortensia" (Matsuno *et al.*, 2008). In recent years, *H. macrophylla* has gained significant attention in the fields of the food industry and pharmacology, primarily due to the presence of dihydroisocoumarins (DHC), hydrangenol (HG), and phylloidalin (PD) (Yasuda *et al.*, 2004). The remarkable chemical diversity inherent in isocoumarins, stemming from their intricate chemical substitution patterns, underlies their extensive range of biological and pharmacological activities. These versatile compounds have been extensively studied and thoroughly documented for their potent antimicrobial, antifungal, insecticidal, antioxidant, anti-cancer, anti-inflammatory, and anti-diabetic properties, as confirmed by research from Tianpanich *et al.* (2011), Das *et al.* (2021), and Krohn *et al.* (2001). Diabetes, a chronic condition resulting from insufficient insulin levels and reduced sensitivity (Bhandari *et al.*, 2008), is characterized by elevated blood sugar levels after meals, especially in type 2 diabetes mellitus (T2DM) (Ch'ng *et al.*, 2019). Controlling elevated blood sugar levels after meals entails regulating the function of enzymes responsible for breaking down carbohydrates within the digestive tract. Two pivotal enzymes in carbohydrate digestion are α -amylase (1,4- α -D-glucan-glucanohydrolase, EC 3.2.1.1) and α -glucosidase (EC 3.2.1.20) (Dona *et al.*, 2010). α -Amylase, a critical enzyme, breaks down complex substances by breaking α -1,4-glucan linkages present in starch, maltodextrins, and similar carbohydrates (Truscheit *et al.*, 2010). α -Glucosidase, which includes maltase, α -dextrinase, and sucrase, is located on the surface of intestinal mucosal cells and cleaves glucose from polysaccharides through hydrolysis of the α -1,4-glycosidic bond. This process aids in the digestion of dietary starch and related carbohydrates, transforming them into absorbable glucose units within the human intestine (Vocadlo *et al.*, 2008).

Moreover, in their 1998 research, Adams *et al.* emphasized the multifaceted nature of DHC, showcasing its broad spectrum of applications in both the food industry and the development of skin-lightening formulations. The primary objective of this study is to conduct a meticulous examination and assessment of the biological activities associated with HG derived from *H. macrophylla* plant leaves. These activities include evaluating its antioxidant capacity, potential anti-diabetic properties, and its ability to inhibit browning processes.

2. MATERIAL and METHODS

2.1. Chemicals

All chemicals were of analytical quality and the solvents for chromatography were of HPLC-grade. HPLC-grade water was produced using a MicroPure instrument (Thermo Electron LED GmbH, Niederelbert, Germany). Moreover, the chemicals were of the highest quality available (95-99%) and were used without purification. Hydrangenol (8-hydroxy-3-(4-hydroxyphenyl)-3,4-dihydroisochromen-1-one, (C₁₅H₁₂O₄)) as reference material was from BOC Sciences, Shirley, USA. The PD (8-hydroxy-3-(3-hydroxy-4-methoxyphenyl)-3,4-dihydro-1H-2-benzopyran-1-one, (C₁₆H₁₄O₅)) was purchased from abcr GmbH, Karlsruhe, Germany. 2,2'-azino-bis-(3-ethylbenzothiazoline-6-sulphonic acid) diammonium salt (ABTS), 2,2'-azobis-(2-amidinopropane) hydrochloride (AAPH), phosphate buffered saline (PBS; pH 7.4, 75 mM), 6-hydroxy-2,5,7,8-tetramethylchroman-2-carboxylic acid (Trolox), HCl and Folin-Ciocalteu phenol reagent (FCR) were obtained from Sigma-Aldrich (Taufkirchen, Germany). Fluorescein and 3, 4, 5-trihydroxybenzoic acid (gallic acid) were bought from Fluka (Buchs, Switzerland). α -Amylase and acarbose were purchased from Sigma-Aldrich, Germany. α -Glucosidase (2000

U) was purchased from NEOGEN Europe Ltd, Scotland, UK, 4-methyl catechol ($C_7H_8O_2$) from Thermo Fisher Scientific GmbH, Dreieich, Germany, p-nitrophenyl- α -D-glucopyranoside ($C_{12}H_{15}NO_8$) from CalbioChem (Merck), Darmstadt, Germany, and Polyvinylpyrrolidone K25 from Sigma, Taufkirchen, Germany, and Triton X-100 ($C_{34}H_{62}O_{11}$) from Riedel-de Haën, Seelze, Germany.

2.2. Description of the Samples

Hydrangea macrophylla leaves were kindly provided by Hansabred GmbH Co. KG (Dresden, Germany). The experimental procedure involved crushing *Hydrangea* leaves in a mortar for 5 minutes. Next, $0.1 \text{ g} \pm 0.01$ of the crushed material was weighed in triplicate and transferred to a 15 mL falcon tube. Subsequently, 2 mL of HPLC water was added, and the mixture was vortexed for 1 minute. The samples were then subjected to fermentation at 70°C for 18 hours using a vacuum oven (Heraeus, Hanau, Germany). After the fermentation process, the samples underwent a 30-minute extraction using 1 mL of MeOH and 1 mL of 70% EtOH in an ultrasonic bath (Sonorex RK 100, Bandelin, Berlin, Germany). Finally, the extraction was followed by centrifugation at 5000 rpm for 5 minutes using a Centrifuge 5702 R (Eppendorf, Hamburg, Germany). The supernatant obtained from the centrifugation was carefully removed and transferred to a 5 mL volumetric flask. The final volume of 5 mL was obtained by adding 70% EtOH. 2 mL of this solution was centrifuged again at 14000 rpm for 5 minutes.

2.3. Identification, Quantification and Isolation

2.3.1. LC-MS/MS analysis

The study followed Ernawita *et al.*'s 2019 separation method, conducted at a constant 30°C temperature using a Kinetex C18 column (150 x 2.1 mm, $5 \mu\text{m}$), Phenomenex Ltd, Aschaffenburg, Germany) preceded by a C18 pre-column. Separation was achieved with a mobile phase of 0.3% formic acid in HPLC water (A) and acetonitrile (B) using a gradient elution profile: starting at 10% A for 2 minutes, increasing to 20% A at 12 minutes, maintaining 35% A from 22 to 25 minutes, and returning to 10% A from 27 to 37 minutes. The flow rate was 0.5 mL/min, and the analysis was conducted at 30°C . Each sample injection used 20 μL , and detection employed a Shimadzu UV detector (Shimadzu, Duisburg, Germany). Qualitative analysis for substance validation was done with the API 2000 MS/MS system in negative ion mode (APCI) (AB Sciex, Darmstadt, Germany) at an evaporation temperature of 400°C . Using Multiple Ion Scan with [M-1]-ions at m/z 285.3 and m/z 255.3, dihydrochalcones (DHC), specifically phyllodulcin and hydrangenol, were confidently identified. Peak assignment in the UV chromatogram was qualitatively performed by comparing mass spectra.

2.3.2. Fractionation

The study employed a specialized preparative HPLC reversed-phase system, including the Merck-Hitachi L-7100 pump, L-7400 UV detector, L-5025 column thermostat, and Shimadzu Chromatopac C-R6A integrator. Separation and fractionation at a column temperature of $20 \pm 1^\circ\text{C}$ utilized a C18 column (250 x 8 mm, Nucleodur, Macherey-Nagel, Düren, Germany), with a mobile phase (flow rate: 4.0 mL/min) of 0.3% formic acid in HPLC-water (A) and acetonitrile (B). The dynamic gradient elution involved 70% A from 0 to 20 minutes, transitioning to 60% A from 20 to 30 minutes, and finally reaching 5% A from 31 to 35 minutes. The injection volume was 800 μL , and detection occurred at 254 nm using a UV detector. Fractionation consisted of repeated isolation and sample collection. These fractions were subsequently concentrated in a rotary evaporator at 30°C under reduced pressure (approximately 20 Pa). The resulting residue was re-dissolved in MeOH and stored at -25°C for further analysis.

2.4. Antioxidants Capacity

2.4.1. Samples preparation

This study focuses on the quantitative evaluation of the antioxidant capacity of HG, which was isolated using preparative HPLC. HG was dissolved in 10 mL ethanol. Dilutions were prepared (factors: 200, 100, 50, 20, 10, and 5) and adjusted to 1 mL with HPLC-grade water.

2.4.2. Determination of total phenolic contents (TP)

In this study, total phenolics (TP) were evaluated in a 96-well microtiter plate using the Folin-Ciocalteu method (Al-Yafeai *et al.*, 2018), a colorimetric oxidation/reduction reaction. Specific components were placed in separate wells: the blank well contained 30 μ L of HPLC water, while other wells held gallic acid monohydrate standard solutions (ranging from 8.51 to 170.12 mg/L) and various dilutions of the HG extract. Subsequently, 150 μ L of Folin-Ciocalteu's 1:10 diluted reagent and 120 μ L of a sodium carbonate solution (75 g/L) were added to each well, ensuring thorough mixing with the samples. The microplate was then shielded from light and incubated at room temperature for 2 hours. After incubation, the absorbance of each sample was measured at 740 nm using a microplate reader set at 30 °C. The total phenolic content was quantified in terms of gallic acid equivalents (GAE) in mg per 100 g of the sample.

2.4.3. Hydrophilic trolox equivalent antioxidant capacity (H-TEAC) assay

Within this investigation, the hydrophilic TEAC assay was utilized, relying on ABTS^{•+} cation radicals. This well-established method for assessing antioxidant radical-quenching capabilities (Al-Yafeai *et al.*, 2018) involved preparing the ABTS^{•+} radical by incubating ABTS and potassium peroxydisulfate solutions. The resulting ABTS^{•+} working solution was freshly diluted with phosphate buffer. In a 96-well microtiter plate, various samples were arranged, including HPLC water (as the blank), Trolox standard at different concentrations, and the methanol/water extract of HG. The HG dilutions were mixed with the ABTS^{•+} working solution, and the reduction in ABTS^{•+} radical absorption at 730 nm due to antioxidant reaction was monitored. Antioxidant capacity was quantified in Trolox equivalents (TE) in mmol per mmol, providing valuable insights into the radical-scavenging potential of the antioxidants.

2.4.4. Hydrophilic oxygen radical absorbance capacity (H-ORAC) assay

The H-ORAC assay, as per Al-Yafeai *et al.* (2018), involves a reaction between the peroxy radical and a fluorescent probe, generating a non-fluorescent product that can be readily quantified using fluorescence. The analysis begins by preparing a fluorescein working solution (1.2 μ M) through a 1:100 dilution of a stock solution of fluorescein (0.12 mM) with phosphate buffer (75 mM, pH 7.4). In a 96-well plate, HG dilutions (10 μ L), the fluorescein working solution (25 μ L), and buffer (100 μ L) are combined. After incubation at 37 °C for 10 minutes, the reaction is started by addition of 150 μ L of a freshly prepared AAPH solution (129 mM). Over 120 minutes at 37 °C, fluorescence intensity is measured (excitation: 490 nm, emission: 510 nm), with readings taken every 60 seconds. To assess antioxidant capacity, we evaluated the rate of non-fluorescent product formation over time. The protective effects of the antioxidants are quantified by calculating the integrated area under the fluorescence decay curves (AUC). Results are expressed in Trolox equivalents (TE) as mmol TE/mmol, providing insights into the antioxidant potential of the tested samples.

2.5. Anti-Diabetic Potential

The study aimed to assess HG's anti-diabetic potential by examining its impact on α -amylase and α -glucosidase activities, with acarbose as a positive control for experimental consistency.

2.5.1. α -Amylase assay

This assay was done according to Ernawita *et al.* (2016), slightly modified. Various control and sample groups were established. The negative control group contained phosphate buffer, starch,

and α -amylase, while the positive control group contained only starch and phosphate buffer. To ensure accuracy and minimize interference, blanks were prepared for each HG serial dilution, consisting of HG dilutions, starch, phosphate buffer, and α -amylase. Isolated HG was dried with nitrogen, re-dissolved in 10 mL of MeOH, and then prepared as triplicate 1 mL samples, which were dried again and re-dissolved in a 10% DMSO and MeOH mixture, generating serial dilutions with phosphate buffer (pH 6.9). Subsequently, 200 μ l of different sample dilutions were combined in 1 mL Eppendorf tubes to prepare test samples and corresponding blank values. Each tube had 400 μ l of starch added and was vortexed for 30 seconds. The tubes were incubated in an orbital shaker at 37 °C for 5 minutes. After incubation, 200 μ l of α -amylase was added to each Eppendorf tube (except for the blank and positive control samples), resulting in a final volume of 800 μ L in each tube. The mixture was vortexed for 30 seconds and further incubated in the orbital shaker at 37 °C for 15 minutes. After the incubation, the solution was transferred into 15 mL plastic tubes containing 800 μ L of HCl. The color reaction was initiated by iodine reagent (1000 μ L). The samples were then transferred to cuvettes, and absorption readings were measured at 630 nm using a spectrophotometer. These meticulous steps allowed for a comprehensive assessment of HG's inhibitory effects on α -amylase activity, indicating its potential as an anti-diabetic agent. The α -amylase inhibitory activity was calculated using Equation (1).

Equation (1):

$$\text{Inhibition of } \alpha\text{-amylase \%} = \left[1 - \left(\frac{A_{630 \text{ blank}} - A_{630 \text{ sample}}}{A_{630 \text{ starch solution}} - A_{630 \text{ negative control}}} \right) \right] * 100$$

2.5.2. α -Glucosidase assay

The experimental procedures in this study involved the utilization of various crucial reagents. A 0.1 M phosphate buffer at pH 6.8 (25 °C) was skillfully prepared by combining two solutions: Solution A (0.2 M $\text{NaH}_2\text{PO}_4 \cdot \text{H}_2\text{O}$) and solution B (0.2 M $\text{Na}_2\text{HPO}_4 \cdot 2\text{H}_2\text{O}$). A p-nitrophenyl- α -D-glucopyranoside (p-NPG) solution at a 2.5 mM concentration was made by dissolving p-NPG in H_2O . Notably, this solution demonstrated stability over two weeks when stored within the temperature range of 0 °C to 5 °C. Additionally, a new enzyme, α -glucosidase (with an activity unit of 120 U/mg and a concentration of 1000 U/mL), was introduced. To maintain consistency in the experimental procedures, the enzyme's activity was adjusted to 0.2 U/mL by dissolving it in a 20 mL phosphate buffer. The inhibition potential of HG on α -glucosidase was evaluated according to Li *et al.*, (2018), with slight adjustments. In this assay, each sample dilution (0.2 mL) was combined with 250 μ L of α -glucosidase (0.25 U/mL) in a pH 6.8 phosphate buffer solution and 500 μ L phosphate buffer, and incubated at 37 °C for 5 minutes. Subsequently, 1 mL of 2.5 mmol/L p-NPG in phosphate buffer solution was added, and the reaction was allowed to proceed for additional 15 minutes at 37 °C. The reaction was stopped with 1 mL of 0.1 mol/L Na_2CO_3 . After further incubation at 37 °C (15 minutes), the absorbance was measured at 405 nm. The α -glucosidase inhibitory activity was calculated using Equation (2).

Equation (2):

$$\text{Inhibition of } \alpha\text{-glucosidase \%} = \left(\frac{A_{405 \text{ control}} - A_{405 \text{ sample}}}{A_{405 \text{ control}}} \right) * 100$$

2.6. Polyphenol Oxidase Activity (PPO)

PPO catalyzes polyphenol oxidation to create colored products. Monitoring 420 nm absorbance changes assesses HG extract effects on PPO activity, offering insights into its significance and inhibition.

2.6.1. Extraction of polyphenol oxidase

In this study, the extraction method as described by Kschonsek *et al.* (2019) was utilized to isolate PPO. The extraction buffer, comprising 0.2 M phosphate buffer (pH 6.5) containing disodium hydrogen phosphate dihydrate (1.272 g), sodium dihydrogen phosphate monohydrate (1.774 g), polyvinylpolypyrrolidone (PvPP) (1 g), and Triton X-100 (250 μ L), with a final volume of 100 mL using HPLC water, was employed. To initiate the extraction process, approximately 2 g \pm 0.015 g of apple samples were precisely weighed in triplicate and transferred to individual 50 mL falcon tubes, maintaining a constant temperature of 4 $^{\circ}$ C. Subsequently, 6 mL of the extraction buffer was added to each tube, ensuring thorough mixing for the uniform distribution of the buffer. The homogenization process was repeated three times for one minute each, using an ultra-turrax operating at 7600 rpm, with the apparatus immersed in an ice bath to maintain low temperatures. After homogenization, the mixture underwent centrifugation at 4 $^{\circ}$ C for 30 minutes at 8000 rpm using a Heraeus Multifuge 1S-R centrifuge. The resulting supernatant was carefully collected and transferred to 15 mL falcon tubes. An additional centrifugation step was then performed for 10 minutes at 4 $^{\circ}$ C and 8000 rpm to ensure the proper separation of the lower phase. The collected lower phase was used for the determination of PPO activity. This passive extraction method effectively retrieved PPO from the samples, providing reliable enzyme activity data for further analysis.

2.6.2. Examination of HG's inhibitory properties on polyphenol oxidase

The inhibitory effect of PPO activity by HG from *H. macrophylla* was investigated using an approach modified from the method described by Bobo *et al.* (2022). HG extracts were prepared at different dilutions (4 mg/mL, 2 mg/mL, and 1 mg/mL) in phosphate buffer by dissolving approximately 40 mg of the extracts in 10% DMSO/MeOH. The experimental setup involved arranging the microplate into specific configurations: (A) A combination of 120 μ L of substrate solution (0.033 M 4-methylcatechol) and 40 μ L of PPO in phosphate buffer (pH 6.8). (B) A blank for the "A" wells, which consisted of 160 μ L of buffer. (C) A mixture of 80 μ L of substrate solution (0.033 M 4-methylcatechol), 40 μ L of HG at different concentrations containing 10% DMSO, and 40 μ L of PPO in phosphate buffer (pH 6.8). (D) A blank for the "C" wells, created by combining 120 μ L of buffer and 40 μ L of the inhibitor. The measurement of PPO activity was initiated immediately after adding the substrate. The enzymatic reaction, converting colorless 4-methylcatechol to orange 4-methyl-o-benzoquinone, was passively monitored by measuring absorbance changes at 420 nm over time at 25 $^{\circ}$ C. This process was executed using the BMG LABTECH FLUOstar OPTIMA plate reader and the Optima computer program (BMG LABTECH, Ortenberg, Germany) for over 100 measurement cycles over a duration of one hour, fifty-seven minutes, and fifteen seconds. Each cycle, lasting 24.75 seconds, included a double orbital shaking of the 96-well plate for one second at 120 rpm before each measurement. To ensure accuracy and reproducibility, all determinations were made in triplicate. Data were analyzed by using the Optima Data Analysis program (BMG LABTECH). An increase in absorbance of 0.001 was considered as 1 unit (U) of enzyme activity. The substrate turnover rate (U/(min*g)) was determined by calculating the slope of the absorption curve within the linear phase of the reaction. The linear phase began a few seconds after adding the substrate and lasted for a brief period before transitioning into a non-linear phase. The extent of PPO inhibition was determined by calculating the percentage of inhibition using Equation (3).

Equation (3):

$$\% \text{ PPO inhibition} = [(((A - B) - (C - D)) / (A - B)) \times 100]$$

3. STATISTICAL ANALYSIS

The data analysis in this study was conducted using Prism program for Windows, version 7.0, developed by GraphPad Software, Inc., San Diego, CA, USA. All experimental analyses were performed in triplicate, and the results are presented as mean \pm standard deviation (SD). To compare data from different analyses, a one-way ANOVA (analysis of variance) followed by the Student-Newman-Keuls post-hoc test (S-N-K) was employed, enabling the identification of significant differences ($p < 0.05$) between multiple groups. Significant differences ($p < 0.05$) between two groups were identified by Paired T-test. Correlations between variables were assessed using Pearson's correlation coefficient (R), with the precision of the methods evaluated using the coefficient of determination (r^2). The relative inhibitory activity (%) and IC50 values were calculated from dose-response inhibition plots created using the GraphPad software, specifically using the dose-response inhibition model (log (inhibitor) vs. normalized response-variable slope).

4. RESULTS

4.1. Quantification and Identification of DHC

The results obtained from the preliminary analysis of *H. macrophylla* leaf extract using chromatography showed multiple peaks at varying retention times. The substances underwent qualitative validation using the API 2000 MS/MS system in negative ion mode (APCI). HG (22.52 min) and PD (24.55 min) were successfully identified through the Multiple Ion Scan with [M-1]⁻ ions at m/z 255.3 and m/z 285.3, respectively. In this study, a calibration curve precisely quantified HG and PD levels, especially at lower concentrations. Consistency is maintained through triplicate analysis, while standard deviation enhanced result reliability, reinforcing the study's robustness. The research uncovers quantitative variations in DHC (HG and PD) content within *H. macrophylla*. Figure 1 shows the levels of HG (192 ± 3 mg/100 g) and PD (37 ± 3 mg/100 g) in a series of examined samples from *H. macrophylla*. The remarkable difference between HG and PD raises questions regarding the determinants affecting DHC levels in *H. macrophylla*.

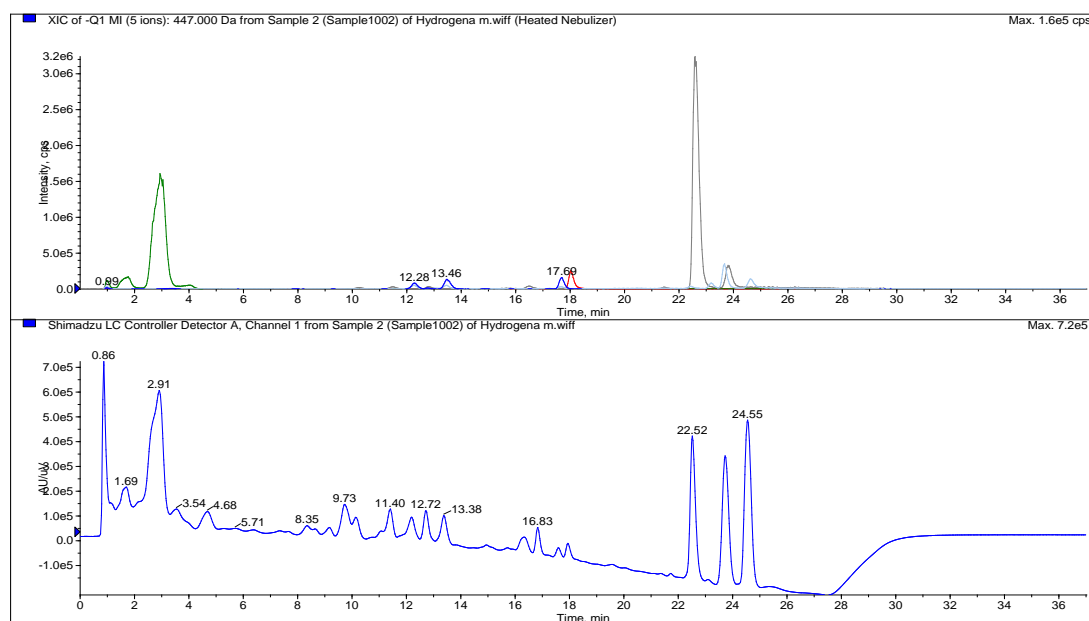


Figure 1. MS and UV chromatograms of *H. macrophylla* leaves extract. The UV analysis was conducted at 214 nm, detecting hydrangenol at 22.52 min and phyllodulcin at 24.55 min.

4.2. Fractionation of DHC

Utilizing preparative HPLC under optimized conditions, HG was successfully extracted from the leaf extract of *H. macrophylla* to ensure optimal purity. Three distinct chromatographic peaks emerged at 15.3, 21.4, and 22.3 minutes, to be further analysed. The identity and purity of HG for the peak at 15.3 minutes was confirmed by LC-MS/MS.

4.3. Biological Activities of HG Isolated from *H. macrophylla* Leaves Extract

4.3.1. Total phenolic contents and hydrophilic antioxidant capacity

In the realm of total phenolics content evaluation, the Folin-Ciocalteu method is employed to harness distinct redox properties. This approach facilitates the quantification of HG's total phenolics content (reducing capacity). The tabulated data within Table 1 illustrate variations in TP levels across diverse dilutions of HG, indicating a statistically significant increase ($p < 0.001$). The highest activity was observed in the factor 100 dilutions, at 11 ± 0.7 g GAE/100 g, while the lowest value was shown in the factor 5 dilutions, measuring 7.0 ± 1.4 g GAE/100 g. In the course of investigating various dilution factors of HG, an intriguing revelation was brought forth: a coefficient of variation of 15% was obtained (Table 1). Notably, the examination of different dilution factors of HG still revealed a significant enhancement in antioxidant capacity, as illustrated in Table 1. Both TEAC and ORAC values continued to exhibit clear increases, with robust statistical analysis confirming the significance of these changes ($p < 0.001$ for TEAC and $p < 0.05$ for ORAC). In a similar vein, the dilution effects were considered to be stronger at a coefficient of variation greater than 10% as presented in Table 1.

Table 1. Total phenolic content and antioxidant capacity of HG in *H. macrophylla* leaf extracts.

Dilution Factor	TP [g GAE/100 g]	H-ORAC [mmol TE/mmol]	H-TEAC [mmol TE/mmol]
200	$9.0 \pm 0.5^{b,c}$	19.0 ± 1.1^a	3.2 ± 0.20^d
100	11.0 ± 0.7^e	25.0 ± 2.1^c	2.3 ± 0.07^c
50	10.0 ± 0.6^d	26.0 ± 2.5^c	2.3 ± 0.03^c
20	9.0 ± 0.1^c	27.0 ± 1.0^c	2.1 ± 0.08^b
10	8.2 ± 0.2^b	$21.0 \pm 1.5^{a,b}$	2.0 ± 0.03^b
5	7.0 ± 1.4^a	15.0 ± 0.1^a	1.7 ± 0.05^a
Mean \pm SD	9.1 ± 1.4	23.0 ± 4.3	2.3 ± 0.5
CV %	15.2	19.1	23.5

The data are presented as mean \pm standard deviation (SD) for three replicates ($n = 3$); along with the coefficient of variation (CV). Significance of differences between samples ($p < 0.05$) was determined using one-way ANOVA followed by the Student-Newman-Keuls post-hoc test, with different letters (a/b/c/d/e) within a column indicating statistically significant distinctions. TP: Total phenolics content, ORAC: Oxygen radical absorbance capacity, TEAC: Trolox equivalent antioxidant capacity, GAE: gallic acid equivalents, TE: Trolox equivalents.

4.3.2. Anti-diabetic potential

Research is currently being conducted to explore compounds that inhibit the enzymes responsible for carbohydrate digestion, with the objective to delay the release of glucose into the bloodstream as a potential strategy for hyperglycemia control. In Figure 2a, the contrasting inhibitory effects of α -amylase activity by acarbose and HG are brought to attention. Acarbose showed an inhibition of 58% with an IC₅₀ of 0.51 mg/mL. Its inhibitory effect was almost linear increasing up to 2.5 mg/mL, eventually reaching 90% inhibition at 10 mg/mL. Conversely, HG displayed significant inhibition, resulting in a 52% reduction with an IC₅₀ of 3.6 mg/mL. These findings highlight concentration-dependent distinctions in their inhibitory capacities.

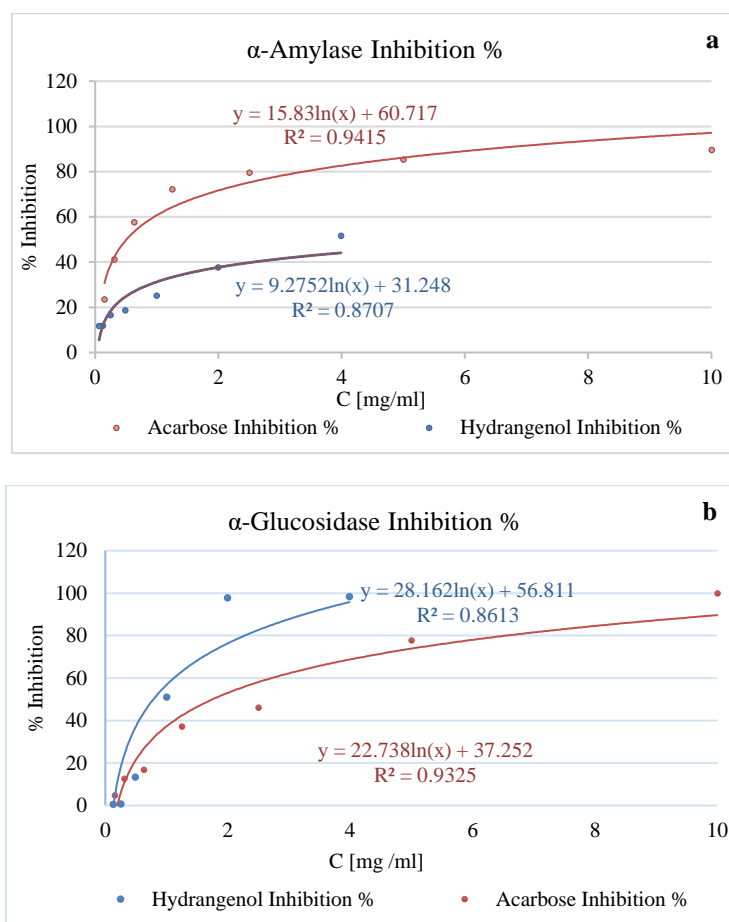


Figure 2. Comparative inhibition effects of HG from *H. macrophylla* leaf extract and acarbose at various concentrations (mg/mL) (a) α -amylase and (b) α -glucosidase.

Furthermore, **Figure 2b** unveils a strikingly consistent inhibition pattern in α -glucosidase activity. Acarbose displayed notable inhibition at 46% with an IC₅₀ of 2.1 mg/mL, characterized by a distinct non-linear trend that captures attention. On the other hand, HG showcased an exceptional inhibition of 51% with an even lower IC₅₀ of 0.97 mg/mL, underscoring its pronounced efficacy in controlling α -glucosidase activity. These results shed light on the potential of HG as a promising candidate for hyperglycemia management.

4.3.3. Anti-browning potential

One goal of this study was to evaluate the potential of HG to inhibit the PPO enzyme, a critical factor regarding food quality and color preservation. The importance of color in consumer choices becomes particularly evident when selecting food items or skincare products. Our investigation has produced significant and noteworthy findings: At concentrations of 1 mg/mL and 2 mg/mL, HG displayed substantial inhibition of PPO activity, with inhibition rates reaching 61%. Conversely, at a concentration of 4 mg/mL, a slightly reduced inhibition rate of 46% on PPO activity was observed. These results emphasize the considerable inhibitory potential of HG in relation to PPO activity, underscoring its promise as a valuable tool for regulating enzymatic browning processes and maintaining the visual appeal of food products (**Table 2**).

Table 2. Inhibitory impact of HG sourced from *H. macrophylla* leaf extracts on PPO activity.

	M ± SD	CV %	Inhibition %
PPO	0.6 ± 0.07	12	
HG 1 mg/mL	0.2 ± 0.02	7	61
HG 2 mg/mL	0.2 ± 0.02	10	61
HG 4 mg/mL	0.3 ± 0.03	11	47

The data are displayed as the mean browning intensity ± standard deviation (SD) across different concentrations in the analysis, accompanied by the coefficient of variation (CV) expressed as a percentage.

5. DISCUSSION and CONCLUSION

The significant difference between the contents of HG and PD in [Figure 1](#) raises questions regarding the factors affecting DHC levels in *H. macrophylla*. The observed fluctuations in DHC levels within *H. macrophylla* could be attributed to two key factors. Firstly, seasonal changes and leaf age, as reported in previous studies, may influence these variations (Moll *et al.*, 2021). Secondly, genetic factors in *H. macrophylla* plants appear to play a crucial role in determining DHC content. Specific genotypes and genetic traits within these plants may be responsible for the observed differences. This genetic influence is further supported by the distribution of HG and PD among various species within the *Hydrangea* genus. HG is found widely across species, while PD is predominantly concentrated in specific species, highlighting the genetic underpinnings of DHC variability. It is plausible that distinct gene sets or clusters regulate the biosynthetic pathways of these compounds, resulting in varying expression levels among different species (Moll *et al.*, 2022).

Within the context of assessing antioxidant capacity and total phenolic contents, this study enhances our comprehension of how the antioxidant efficacy of HG is impacted by diverse dilution factors, providing insights into its performance under varying conditions. HG, a naturally occurring dihydroflavonol classified within the flavonoid subgroup, assumes a pivotal role in antioxidant functions. Flavonoids, such as HG, possess the capability to counteract reactive oxygen species, a fundamental mechanism contributing to their antioxidant potential. This is achieved through two primary pathways: the immediate neutralization of free radicals via hydrogen atom donation and participation in single-electron transfer reactions (Procházková *et al.*, 2011). Another notable attribute of flavonoids lies in their capacity to chelate transition metal elements. By forming chelates with metal ions in the human body, flavonoids effectively shield these ions from oxidation. Specific flavonoids can also chelate trace metal ions like Fe²⁺ and Cu⁺, which play essential roles in oxygen metabolism and free radical formation (Malešev & Kunti 2007). Moreover, the observation that the coefficient of variation was higher than 10%, as demonstrated in [Table 1](#), is noteworthy. This result is in accordance with the findings reported by Hengst *et al.* (2009), adding further support to the idea that a coefficient of variation exceeding 10% indicates a substantial impact of the dilution factor on antioxidant capacity. This observation is consistent with the research of Híc and Balík (2012), reaffirming that the dilution factors of materials have indeed influenced the results.

Acarbose, originating as a fermentation byproduct of actinoplanes species, functions as a competitive inhibitor targeting both α -amylase and α -glucosidase enzymes. Its primary role centers on the management of type 2 diabetes, achieved by effectively impeding the activity of glucosidases present in the upper gastrointestinal tract (Kim *et al.*, 1999). This inhibitory effect is dosage-dependent, resulting in delayed absorption of glucose and a reduction in postprandial hyperglycemia. However, the administration of acarbose is often associated with gastrointestinal side effects, predominantly characterized by flatulence, and on occasion, instances of soft stools or abdominal discomfort (Rosak and Mertes, 2012). Research is

exploring compounds that inhibit carbohydrate-digesting enzymes to delay glucose release into the bloodstream, a potential strategy for controlling hyperglycemia.

The inhibitory effects against α -amylase and α -glucosidase, as observed in this study, align with the findings of Li *et al.* (2018), who also reported similar outcomes for flavonoid-rich extracts. Highlighting the distinctions between acarbose and HG enhances our understanding of complex interaction dynamics, enriching our comprehension of enzymatic inhibition mechanisms and their broader implications in the biological context.

Enzyme inhibitors, chemical compounds that hinder or completely suppress enzymatic catalysis, come in different types. Reversible apoenzyme inhibitors, for instance, fall into three categories: competitive, uncompetitive, and noncompetitive (or mixed-type) (Sharma, 2012). Uncompetitive inhibitors bind to a site on the enzyme-substrate complex being different from the substrate's site. Competitive inhibitors, on the other hand, occupy the same site as the substrate on the enzyme. Mixed inhibitors interact with both the enzyme and the enzyme-substrate complex. In the non-competitive or mixed mechanism, the enzyme undergoes a conformational change into an inactive state, leading to an inability to bind to the substrate or release the product. The competitive mechanism in contrast involves the reversible blockage of the active site, preventing substrate molecules from binding (Nelson & Cox, 2005).

The inhibitory effectiveness of phenolic compounds in various modes (mixed, uncompetitive, competitive) is intricately linked to their molecular structures (Kim *et al.*, 2009). Phenolic acids' inhibitory potential is heavily influenced by the presence of hydroxyl and methoxy groups within their aromatic ring (Malunga *et al.*, 2018). In contrast, flavonoids, with additional hydroxyl groups, exhibit superior inhibition of α -glucosidase activity (Di Stefano *et al.*, 2018). The introduction of more aromatic hydroxyl groups through glucoside substitutions further enhances enzyme inhibition (Şöhretoğlu *et al.*, 2018). Molecular docking studies indicate that phenolic compounds establish interactions with both active and allosteric sites, primarily through hydrogen bonding, hydrophobic interactions, and van der Waals forces, facilitating their binding with enzymes (Di Stefano *et al.*, 2018). It's worth noting that p-coumaric acids are notably effective in inhibiting α -glucosidase through mixed noncompetitive inhibition (Li *et al.*, 2009).

Enzymatic browning, common in fruits and vegetables, results from the oxidation of phenolic compounds catalyzed by the PPO enzyme. Tyrosinase, a key enzyme, triggers this process when it interacts with polyphenols in the presence of oxygen, disrupting cell structure. The PPO enzyme is classified into two categories: EC1.14.28.1 (tyrosinase, cresolase, and monophenol monooxygenase) and EC1.10.3.1 (o-diphenol oxygen oxidoreductase, diphenol oxidase, and catechol oxidase) (Moon *et al.*, 2020; Mayer, 2006; Hurrel & Finot, 1984). Simultaneously, roughly 15% of the global population utilizes skin-whitening agents to diminish melanin production, the pigment responsible for skin color and protection against UV radiation. Nevertheless, the excessive accumulation of melanin stemming from factors like UV exposure and certain medications can lead to the formation of pigmented patches, giving rise to aesthetic concerns (Loizzo *et al.*, 2012 and Briganti *et al.*, 2003).

These results illustrate the temporal dynamics of browning intensity. The tabulated data accentuates the prominent inhibitory efficacy of HG in relation to PPO activity, thereby emphasizing its potential utility as a modulator of enzymatic browning processes. Within the domain of the flavonoid subclass, HG manifests as an inherent dihydroflavonol, characterized by the presence of hydroxyl groups, thereby assuming a central regulatory position in anti-browning mechanisms. Notably, these polyphenols boast hydroxyl groups that can engage in electron donation to intermediate quinones, effectively impeding the oxidation process. Furthermore, enzymes stemming from phenolic compounds exhibit the ability to chelate metal ions, particularly Cu^{2+} , at both binding and catalytic sites of the PPO enzyme. Consequently,

the formation of hydrogen bonds between these phenolic derivatives and the active sites of enzymes leads to a reduction in enzyme activity (Sae-leaw *et al.*, 2019).

In summary, this study thoroughly investigated the biological potential of hydrangenol, a key bioactive compound derived from *Hydrangea macrophylla*. Employing rigorous analytical techniques and varying hydrangenol concentrations, the research revealed significant antioxidant properties and notable enzyme inhibition activities, including anti-diabetic and anti-browning effects. These results feature the manifold applications of hydrangenol across various scientific fields. As a result, this research provides a solid foundation for future investigations in this scientific area.

Acknowledgments

Authors gratefully acknowledge the Friedrich Schiller University Jena for the 603 scholarship (Scholarships for female postdoctoral researchers) funding of Ahlam Al-Yafeai.

Declaration of Conflicting Interests and Ethics

The authors declare no conflict of interest. This research study complies with research and publishing ethics. The scientific and legal responsibility for manuscripts published in IJSM belongs to the authors.

Authorship Contribution Statement

Ahlam Al-Yafeai: Conception and experimental design, Experiment execution (LC-MS/MS analysis), Fractionation and anti-diabetic potential, Evaluation (antioxidant capacity, PPO), Manuscript preparation and data analysis, Manuscript review and editing. **Barbara Schmitt:** Fractionation and anti-diabetic potential. **Angelika Malarski:** Experiment execution (LC-MS/MS analysis). **Volker Böhm:** Conception and experimental design, Manuscript review and editing.

Orcid

Ahlam Al-Yafeai  <https://orcid.org/0009-0003-3095-3574>

Barbara Schmitt  <https://orcid.org/0009-0004-4823-9720>

Angelika Malarski  <https://orcid.org/0009-0006-5986-5000>

Volker Böhm  <https://orcid.org/0000-0002-9474-4718>

REFERENCES

- Abbas, M., Saeed, F., & Anjum, F.M. (2017). Natural polyphenols: An overview. *Int. J. Food Prop.*, 20, 1689-99. <http://dx.doi.org/10.1080/10942912.2016.1220393>
- Adams, T.B., Greer, D.B., Doull, J., Munro, I.C., Newberne, P., Portoghese, P.S., Smith, R.L., Wagner, B.M., Weil, C.S., Woods, L.A., & Ford, R.A. (1998). The FEMA GRAS assessment of lactones used as flavour ingredients. *Food and Chemical Toxicology*, 36, 249-278. [https://doi.org/10.1016/s0278-6915\(97\)00163-4](https://doi.org/10.1016/s0278-6915(97)00163-4)
- Al-Yafeai, A., Bellstedt, P., & Böhm, V. (2018). Bioactive compounds and antioxidant of *Rosa rugosa* depending on degree of ripeness. *Antioxidants*, 7, 134. <https://doi.org/10.3390/antiox7100134>
- Bhandari, M.R., Jong-Anurakkun, N., Hong, G., & Kawabata, J. (2008). α -Glucosidase and α -amylase inhibitory effects of Nepalese medicinal herb Pakhanbhed (*Bergenia ciliata*, Haw.). *Food Chem.*, 106, 247-252. <https://doi.org/10.1016/j.foodchem.2007.05.077>
- Bobo, G., Arroqui, & Virseda, P. (2022). Natural plant extracts as inhibitors of potato polyphenol oxidase: The green tea case study. *LWT - Food Science and Technology*, 153, 112467. <https://doi.org/10.1016/j.lwt.2021.112467>
- Briganti, S., Camera, E., & Picardo, M. (2003). Chemical and instrumental approaches to treat hyperpigmentation. *Pigment Cell Research*, 16(2), 101-110. <http://dx.doi.org/10.1034/j.1600-0749.2003.00029.x>

- Ch'ng, L.Z., Barakatun-Nisak, M.Y., Zukiman, W.Z.H.W., Abas, F., & Wahab, N.A. (2019). Nutritional strategies in managing postmeal glucose for type 2 diabetes: A narrative review. *Diabetes & Metabolic Syndrome: Clinical Research & Reviews.*, *13*, 2339-2345. <https://doi.org/10.1016/j.dsx.2019.05.026>
- Das, V., Kaishap, P.P., Duarah, G., Chikkaputtaiah, C., Deka Boruah, H.P., & Pal, M. (2021). Cytotoxic and apoptosis-inducing effects of novel 8-amido isocoumarin derivatives against breast cancer cells. *Naunyn-Schmiedeb. Naunyn-Schmiedeberg's Arch. Pharmacol.*, *394*, 1437-1449. <https://doi.org/10.1007/s00210-021-02063-9>
- Di Stefano, E., Oliviero, T., & Udenigwe, C.C. (2018). Functional significance and structure–activity relationship of food-derived α -glucosidase inhibitors. *Current Opinion in Food Science*, *20*, 7-12. <https://doi.org/10.1016/j.cofs.2018.02.008>
- Dona, A.C., Pages, G., Gilbert, R.G., & Kuchel, P.W. (2010). Digestion of starch: *In vivo* and *in vitro* kinetic models used to characterize oligosaccharide or glucose release. *Carbohydrate Polymers*, *80*, 599-617. <https://doi.org/10.1016/j.carbpol.2010.01.002>
- Ernawita, Thieme, C., Westphal, A., Malarski, A., & Böhm, V. (2019). Polyphenols, vitamin C, *in vitro* antioxidant capacity, α -amylase and COX-2 inhibitory activities of citrus samples from Aceh, Indonesia. *Int. J. Vitam. Nutr. Res.*, *89*, 337-347. <https://doi.org/10.1024/0300-9831/a000481>
- Ernawita, Wahyuono, R.A., Hesse, J., Hipler, U.-C.; Elsner, P., & Böhm, V. (2016). Carotenoids of indigenous citrus species from Aceh and its *in vitro* antioxidant, antidiabetic and antibacterial activities, *European Food Research and Technology*, *242*, 1869-1881. <https://doi.org/10.1007/s00217-016-2686-0>
- Gianmaria, F., Ivana, A., Aniello, I., Armando, Z., Gabriele, P., & Antonino, P. (2011). Plant polyphenols and their anti-cariogenic properties, *Molecules*, *16*, 1486-1507. <https://doi.org/10.3390/molecules16021486>
- Hengst, C., Werner, S., Müller, L., Fröhlich, K., & Böhm, V. (2009). Determination of the antioxidant capacity: Influence of the sample concentration on the measured values. *European Food Research and Technology*, *230*, 249–254. <https://doi.org/10.1007/s00217-009-1166-1>
- Hic, P., & Balik, J. (2012). Effect of sample dilution on estimated values of antioxidant capacity by photochemiluminescence method. *Acta Univ. Agric.Silvic. Mendel. Brun.*, *8*, 67-72. <https://doi.org/10.11118/actaun201260080067>
- Hurrell, R.F. and Finot, P.A. (1984). Nutritional consequences of the reactions between proteins and oxidised polyphenolic acids. *Adv. Exp. Med. Biol.*, *177*, 423-35.
- Kim, J.H., Kim, H.Y., & Jin, C.H. (2009). Mechanistic investigation of anthocyanidin derivatives as alpha-glucosidase inhibitors. *Bioorganic Chemistry*, *87*, 803-809. <https://doi.org/10.1016/j.bioorg.2019.01.033>
- Kim, M.J., Lee, S.B., Lee, H.S., Lee, S.Y., Baek, J.S., Kim, D., Moon, T.W., Robyt, J.F., & Park, K.H. (1999). Comparative study of the inhibition of alpha-glucosidase, alpha-amylase, and cyclomalto-dextrin glucanotransferase by acarbose, isoacarboses, and acarviosine-glucose. *Archives of Biochemistry and Biophysics*, *371*, 277-283. <https://doi.org/10.1006/abbi.1999.1423>
- Krohn, K., Flörke, U., Rao, M.S., Steingröver, K., Aust, H.J., Draeger, S., & Schulz, B. (2001). Metabolites from fungi 15. New isocoumarins from an endophytic fungus isolated from the Canadian thistle *Cirsium arvense*. *Natural Product Letters*, *15*, 353-361. <https://doi.org/10.1080/10575630108041303>
- Kschonsek, J., Wiegand, C., Hipler, U.-C., & Böhm, V. (2019). Influence of polyphenolic content on the *in vitro* allergenicity of old and new apple cultivars: A pilot study. *Nutrition*, *58*, 30-35. <https://doi.org/10.1016/j.nut.2018.07.001>

- Li, K., Fan, H., Yin, P.P., Yang, L.G., Xue, Q., Li, X.; Sun, L.W., & Liu, Y.J. (2018). Structure activity relationship of eight primary flavonoids analyzed with a preliminary assign-score method and their contribution to antioxidant ability of flavonoids-rich extract from *Scutellaria baicalensis* shoots. *Arabian Journal of Chemistry*, *11*, 159-170. <https://doi.org/10.1016/j.arabjc.2017.08.002>
- Li, K., Yao, F., Xue, Q., Fan, H., Yang, L., Li, X., Sun, L., & Li, Y. (2018). Inhibitory effects against α -glucosidase and α -amylase of the flavonoids-rich extract from *Scutellaria baicalensis* shoots and interpretation of structure-activity relationship of its eight flavonoids by a refined assign-score method. *Chemistry Central Journal*, *12*, 82. <https://doi.org/10.1186/s13065-018-0445-y>
- Li, Y.Q., Zhou, F.C., & Gao, F.(2009). Comparative evaluation of quercetin, isoquercetin and rutin as inhibitors of α -glucosidase. *J. Agric. Food Chem.* *57*(24), 11463-11468. <https://doi.org/10.1021/jf903083h>
- Loizzo, M.R., Tundis, R., & Menichini, F. (2012). Natural and synthetic tyrosinase inhibitors as antibrowning agents: an update. *Compr. Rev. Food Sci. Food Saf.*, *11*, 378-398. <http://dx.doi.org/10.1111/j.1541-4337.2012.00191.x>
- Malešev, D., & Kunti, V.(2007). Investigation of metal-flavonoid chelates and the determination of flavonoids via metal-flavonoid complexing reactions. *J. Serb. Chem. Soc.*, *72*, 921-939. <https://doi.org/10.2298/JSC0710921M>
- Malunga, L.N., Thandapilly, S.J., & Ames, N. (2018). Cereal-derived phenolic acids and intestinal alpha glucosidase activity inhibition: Structural activity relationship. *Journal of Food Biochemistry*, *42*, e12635. <https://doi.org/10.1111/jfbc.12635>
- Matsuno, T., Kunikate, T., Tanigawa, T., Suyama, T., & Yamada, A. (2008). Establishment of cultivation system based on flowering characteristics in *Hydrangea serrata* (Thunb.) Ser. *Hortic. Res.*, *7*, 189-195. <https://doi.org/10.2503/hrj.7.189>
- Mayer, A.M. (2006). Polyphenol oxidases in plants and fungi: going places? *Phytochemistry*, *67*, 2318-31. <https://doi.org/10.1016/j.phytochem.2006.08.006>
- Moll, M.D., Kahlert, L., Gross, E., Schwarze, E.-C., Blings, M., Hillebrand, S., Ley, J., Kraska, T., & Pude, R. (2022). VIS-NIR modeling of hydrangenol and phyllodulcin contents in tea-hortensia (*Hydrangea macrophylla* subsp. *serrata*), *Hortic.*, *8*, 264. <https://doi.org/10.3390/horticulturae8030264>
- Moll, M.D., Tränkner, C., Blings, M., Schwarze, E.-C., Gross, E., Hillebrand, S., Ley, J., Kraska, T., & Pude, R. (2022). Proposing a chemometric normalized difference phyllodulcin index (cNDPI) for phyllodulcin synthesis estimation, *J. JARMAP*, *30*, 100398. <https://doi.org/10.1016/j.jarmap.2022.100398>
- Moll, M.D., Vieregge, A.S., Wiesbaum, C., Blings, M., Vana, F., Hillebrand, S., Ley, J., Kraska, T., & Pude, R. (2021). Dihydroisocoumarin content and phenotyping of *Hydrangea macrophylla* subsp. *serrata* cultivars under different shading regimes. *Agronomy*, *11*, 1743. <https://doi.org/10.3390/agronomy11091743>
- Moon, K.M., Kwon, E.B., Lee, B., & Kim, C.Y. (2020). Recent trends in controlling the enzymatic browning of fruit and vegetable products. *Molecules*, *25*, 2754. <https://doi.org/10.3390/molecules25122754>
- Nelson, D., & Cox, M. (2005). Enzyme kinetics as an approach to understanding mechanism. In *Lehninger Principles of Biochemistry*, 4th ed.; Freeman, W.H., Ed.; Macmillan: New York, NY, USA.
- Procházková, D., Bousová, I., & Wilhelmová, N. (2011). Antioxidant and prooxidant properties of flavonoids. *Fitoterapia*, *82*, 513-523. <https://doi.org/10.1016/j.fitote.2011.01.018>
- Rosak, C., & Mertes, G. (2012). Critical evaluation of the role of acarbose in the treatment of diabetes: patient considerations. *Diabetes, Metabolic Syndrome and Obesity*, *5*, 357-367. <https://doi.org/10.2147/DMSO.S28340>

- Sae-leaw, T., & Benjakul, S. (2019). Prevention of melanosis in crustaceans by plant polyphenols: A review. *Trends in Food Science & Technology*, 85, 1-9. <https://doi.org/10.1016/j.tifs.2018.12.003>
- Sharma, R. (2012). Enzyme inhibition and bioapplications; *IntechOpen*: Rijeka, Croatia, <https://doi.org/10.5772/1963>
- Singh, P., & Goyal, G.K. (2008). Dietary lycopene: Its properties and anticarcinogenic effects. *Compr. Rev. Food Sci. Food Saf.*, 7, 255-270. <https://doi.org/10.1111/j.1541-4337.2008.00044.x>
- Suzuki, H., Ikeda, T., Matsumoto, T., & Noguchi, M. (1978). Polyphenol components in cultured cells of amacha (*Hydrangea macrophylla* Seringe var. thunbergii Makino). *J-STAGE*, 42, 1133-1137. <https://doi.org/10.1080/00021369.1978.10863124>
- Şöhretoğlu, D., Sari, S., Barut, B., & Özel, A. (2018). Discovery of potent α -glucosidase inhibitor flavonols: Insights into mechanism of action through inhibition kinetics and docking simulations. *Bioorganic Chemistry*, 79, 257-264. <https://doi.org/10.1016/j.bioorg.2018.05.010>
- Tianpanich, K., Prachya, S., Wiyakrutta, S., Mahidol, C., Ruchirawat, S., & Kittakoop, P.J. (2011). Radical scavenging and antioxidant activities of isocoumarins and a phthalide from the endophytic fungus *Colletotrichum* sp. *J. Nat. Prod.*, 74, 79-81. <https://doi.org/10.1021/np1003752>
- Truscheit, E., Frommer, W., Junge, B., Müller, L., Schmidt, D.D., & Wingender, W. (2010). Chemistry and biochemistry of microbial α -glucosidase inhibitors. *Angewandte Chemie International Edition in English*, 20, 744-761
- Vocadlo, D.J., & Davies, G.J. (2008) Mechanistic insights into glycosidase chemistry. *Curr. Opin. Chem. Biol.*, 12, 539-555. <https://doi.org/10.1016/j.cbpa.2008.05.010>
- Yasuda, T., Kayaba, S., Takahashi, K., Nakazawa, T., & Ohsawa, K. (2004). Metabolic fate of orally administered phyllodulcin in rats. *J. Nat. Prod.*, 67, 1604-1607. <https://doi.org/10.1021/np0400353>